Verification of the RAMS-based Operational Weather Forecast System in the Valencia Region: a seasonal comparison

I. GÓMEZ[a], M. J. ESTRELA[b,c], V. CASELLES[a,c]

(Natural Hazards, 2015, 75(2): 1941-1958. DOI: 10.1007/s11069-014-1408-9: http://link.springer.com/article/10.1007%2Fs11069-014-1408-9)

[a] *Departament de Física de la Terra i Termodinàmica, Facultat de Física, Universitat de València, Doctor Moliner, 50, 46100 Burjassot, Valencia, Spain.*

[b] *Departament de Geografia, Facultat de Geografia i Història, Universitat de València, Avda. Blasco Ibáñez, 28, 46010 Valencia, Spain.*

[c] *Laboratorio de Meteorología y Climatología, Unidad Mixta CEAM-UVEG, Charles R. Darwin, 14, 46980 Paterna, Valencia, Spain.*

Correspondence to: Igor Gómez Doménech

E-mail: godoi@uv.es

ABSTRACT

The meteorological model Regional Atmospheric Modeling System (RAMS) in its version 4.4 has been applied operationally within the Valencia Region. The model output is being used as support for a heat-wave warning system, a wind forecasting system for fire warnings and prevention, and for general forecasting tasks. For the winter period of 2010-2011 and the summer period of 2011, the model version 6.0 has been included within the operational forecast environment. In this study, the verification of the model using both versions has been performed taking advantage of the automatic weather stations from the CEAM network and located within this area. Surface meteorological observations have been compared with the RAMS forecasts in an operational verification focused on computing different statistical data for coastal and inland stations. This verification process has been carried out both for the summer and the winter seasons of the year separately. As a result, it has been revealed that the model presents significant differences in the forecast of the meteorological variables analysed throughout both periods of the year. Moreover, the model presents different degrees of accuracy between coastal and inland stations as well as for both versions of RAMS for the meteorological variables investigated. On the other hand, we have also found that there is little difference in the magnitudes analyzed within the two daily RAMS cycles and that RAMS is very stable in maintaining skilful forecast results at least for three forecast days, although the performance of the simulation slightly decreases as the simulation moves forward.

Keywords: RAMS model, operational forecasting, mesoscale modelling, model verification, numerical weather prediction, natural hazards, warning and alert systems.

1. Introduction

The Valencia Region, located in the Western Mediterranean Basin, due to its geographical position and its climatic and physical characteristics, has a significant meteorological interest as it is especially sensitive to certain severe weather events such as torrential rain (Millán et al., 1995; Pastor et al., 2001; Estrela et al, 2002; Pastor et al., 2010; Gómez et al., 2011), forest fires (Gómez-Tejedor et al., 1999) or heat waves (Miró et al., 2006; Estrela et al., 2007; Gómez et al., 2010; Gómez et al., 2013). The east part of the Valencia Region is bordered by the Mediterranean Sea, while not far from the coast and more inland, mountain ranges are found exceeding 1500 m in height (Fig. 1). The terrain of the Western Mediterranean Basin exerts a strong influence on its weather regimes by generating local and regional mesoscale circulations on diurnal time scales (Millán et al., 1997, Gangoiti et al., 2001). Thus, the Valencia Region combines the difficulty of land-sea contrasts, mountainous terrain and large-scale mesoscale circulations (Pérez-Landa et al. 2007).

Under summertime conditions, a marked diurnal cycle of the wind direction and pressure is observed in the Valencia Region (Pérez-Landa et al. 2007; Azorin-Molina et al., 2008; Azorin-Molina et al., 2011). This period is characterized by a nocturnal drainage flow with katabatic winds chanelled by the valleys, a combined breeze regime during which the sea breeze merges with convective uplift over the mountain ranges followed by a subsiding flow over the sea, and an evening regime where a large inland pressure can interact with the combined breeze and change the flow pattern (Pérez-Landa et al. 2007, Salvador et al. 1997). During the warm period, high summer temperatures over this region are observed, permitting record maximum temperatures exceeding 30ºC, as well as record low temperatures exceeding 20ºC, during so-called tropical nights (Estrela et al., 2007, Miró et al. 2006).

Under winter conditions, Atlantic frontal systems crossing the Iberian Peninsula dominates, together with the migration of high pressure areas towards the center of the continent. The movement of these high pressure areas towards the east provokes the entrance of cold continental air over the Mediterranean (Millán et al., 2005). During the cold period of the year, the Valencia Region is affected by low temperatures, mainly related to the entrance of northerly arctic air, entrance of northeasterly continental polar air or anticyclonic situations. Besides, strong radiative cooling of the ground and the corresponding surface temperature inversion are also found in valleys and flat areas over the Valencia Region, specially located inland. This situation produces very low temperatures, but located in specific areas affected by thermal inversion phenomenon. Finally, the entrance of northwesterly air can cause relatively low temperatures, but in principle this kind of situation is not responsible for very low temperatures over this region.

Taking into account the sensitivity of the Valencia Region to climate hazards, the use of a mesoscale model operating at high resolution would be useful as a warning forecasting tool. In this sense, a meteorological real-time forecasting system was designed and implemented at the CEAM (Centro de Estudios Ambientales de Mediterráneo; Mediterranean Center for Environmental Studies) Foundation (Gómez et al., 2010), based on the Regional Atmospheric Modeling System (RAMS) (Pielke et al., 2002; Cotton et al., 2003).

The aim of the current work is to investigate the skill of the RAMS model within the operational weather forecasting system implemented for the Valencia Region

(Gómez et al., 2010). For this, we have taken advantage of the available data on this area. It consists of near-surface meteorological observations provided by the CEAM weather stations network. In order to achieve a comprehensive description of the performance of the RAMS model, the verification process has been developed by dividing the available information into three steps. Firstly, instead of performing a verification of the model for the whole year, we have separated winter and summer. Due to the fact that the dominant wintertime meteorological processes are different from those observed in the summertime over the area of study (Miró et al., 2009), this division between both seasons of the year will provide a more detailed picture of the RAMS results within the Valencia Region. In addition, it will be helpful to detect differences that could appear between both periods of the year. Secondly, RAMS in its version 6.0, has been implemented for the winter of 2010-2011 and the summer of 2011, simultaneously with the version 4.4, within the operational forecasting system (Gómez et al., 2010). These two seasons are used in this study to operate a correlative verification process for both seasons of the year separately. As a result, the corresponding simulations acquire a description of the differences between the most recent versions of the model. In Miró et al. (2009), they developed a methodology to automatically identify and characterize the daily atmospheric situation for the period of 1958-2008. Applying the same approach to the winter of 2010-2011 and the summer of 2011, we have examined to what degree these specific seasons vary from the typical prevailing in the region, considering the original time interval 1958-2008. As a result, it has been found that the percentage of occurrence of the distinct meteorological situations that this procedure detects is similar when using the whole climatic period separating winter from summertime than when using the winter of 2010-2011 and the summer of 2011 independently. Thus, it may be said that these particular seasons follow the typical patterns prevailing in the Valencia Region (Miró et al., 2009). In the third place, coastal stations have been isolated from inland ones, to evaluate differences between station locations, as it was already done by Gómez et al. (2013).

The paper is structured as follows: section 2 presents the model configuration, as well as the observational data used in this study and the verification procedure. The results of the verification procedure are given in section 3. Finally, section 4 is devoted to the conclusions of this work.

2. Data and verification methodology

2.1. RAMS model

RAMS model in its version 4.4 (RAMS44) and 6.0 (RAMS60) has been used in this study (Pielke et al., 2002; Cotton et al., 2003). The current RAMS set-up includes the Mellor and Yamada (1982) level 2.5 turbulence parameterization, a full-column two-stream single-band radiation scheme that accounts for clouds and calculates short-wave and long-wave radiation (Chen and Cotton, 1983), and the cloud and precipitation microphysics scheme from Walko et al. (1995), applied in all the domains. The Kuo-modified parameterization of sub-grid scale convection processes is used in the coarse domain (Molinari et al., 1985), whereas grids 2 and 3 utilize explicit convection only. Finally, the LEAF-2 soil-vegetation surface scheme (Walko et al., 2000) is used within the RAMS44 environment while LEAF-3 is used for RAMS60. This parameterization permits to calculate sensible and latent heat fluxes exchanged within the atmosphere, using prognostic equations for soil moisture and temperature. The main improvement in developing LEAF-3 from LEAF-2 was to input the Normalized Difference Vegetation Index (NDVI) and use it to compute essential vegetation characteristics of different vegetation parameters. The NDVI value provides valuable information on the spatial and temporal variability of greenness, which is absent from the simple model used in LEAF-2. A detailed description of the diverse changes performed is included in Walko et al. (2005).

In the current CEAM RAMS implementation, the following two-way interactive nesting domain configuration (Fig. 1) is used: Grid 1 covers the southern part of Europe at a 48-km horizontal grid resolution and a large part of the Mediterranean basin, Grid 2 covers the Iberian Peninsula and the Western Mediterranean with a grid resolution of 12 km, and a high resolution domain (3 km) (Grid 3), includes the Valencia Region. In the vertical, a 24-level stretched scheme has been selected, with a 50-m space near the surface increasing gradually up to 1,000 m near the model top at 11,000 m and with 9 levels in the lower 1,000 m. A summary of the horizontal and vertical grid parameters is provided in Table 1. The lowest model level of this configuration is located approximately 24 m above the ground. This configuration was selected from different sensitivity exercises (Unpublished work) as the best compromise for resolving the mesoscale circulations in the Valencia Region within a time frame regarded as useful for the model forecast, considering the available computational resources.

RAMS initial and boundary conditions are derived from the operational global model of the National Centre for Environmental Prediction (NCEP) Global Forecasting System (GFS), at 6 hr intervals and 1 x 1 degree resolution globally, using a Four-Dimensional Data Assimilation (FDDA) technique applied to define the forcing at the lateral boundaries of the outermost five grid cells of the largest domain. In this sense, we are nudging toward the GFS gridded data, where the nudging time scale at the lateral boundary corresponds to 900 seconds for each operational cycle. Weather forecasts are performed twice a day, at 0000 and 1200 UTC, for RAMS44 and RAMS60, using the GFS forecast grid from its forecast cycle 12-h earlier, and for a forecast range of three complete days (today, tomorrow and the day after tomorrow). RAMS forecast outputs are available once every hour for display and analysis purposes.

2.2. Observational data

A total of 6 automatic surface weather stations from the CEAM network have been used to perform the verification of the RAMS results (2 corresponding to coastal locations and 4 corresponding to inland ones) (Fig. 1). These representative stations for coastal and inland locations are used to show the model skill focused on specific areas within the Valencia Region (Gómez et al., 2013). Although the CEAM weather stations network stores data in a 10-minute basis, hourly-mean measures of near-surface temperature, relative humidity and wind speed and direction from this network have been used in the verification process, in order to match the RAMS output frequency.

2.3. Verification procedure

To analyse the RAMS results, we have followed a procedure that uses the simulated results obtained with the higher resolution domain to account for the terrain influence on the atmospheric flows (Salvador et al., 1999). We have developed a software tool to extract and store, for each daily simulation within the period of study (The winter of 2010-2011 and summer of 2011), diverse hourly RAMS forecasted magnitudes. On the one hand, we saved the near-surface temperature, relative humidity, wind speed and direction, at each selected CEAM station location using Grid 3 (Fig. 1). This surface data has been stored in a database for the three days of simulation and for the two RAMS versions. On the other hand, as only surface measurements are available for this model verification, besides the near-surface RAMS variables, other relevant magnitudes such as the 2-m temperature and the 10-m wind speed were saved in the same terms. Therefore, both forecasting products are evaluated by comparing them with the observations which are available at the specific sensor height. This may be helpful in order to investigate which of these variables represents the meteorological patterns reproduced by the observations more accurately.

The software developed to evaluate the RAMS model uses the RAMS/HYPACT Evaluation and Visualization Utilities (REVU) software (Tremback et al., 2002) applied to Grid 3. Specifying the latitude, longitude and sensor height for each observational location, REVU interpolates forecast data in three dimensions from surrounding RAMS grid points. For sensor heights below the first model physical level, REVU vertically interpolates between the belowground computational level and the first physical level above ground rather than performing similarity theory calculations (Case et al., 2002). In this sense, the simulated near-surface variables have been interpolated to the corresponding sensor height for each observational location.

Separate processes are carried out in the RAMS verification. A series of statistical scores have been computed for each CEAM station and for each simulation hour independently (Willmott, 1981; Pielke, 2002; Palau et al. 2005; Pérez-Landa et al., 2007). The statistical calculations carried out in both cases include the mean bias, root mean square error (RMSE) and index of agreement (IoA) for temperature, relative humidity and wind speed. The IoA is a modified correlation coefficient that measures the degree to which a model's prediction is free of error (Willmott, 1981). A value of 0 means complete disagreement while a value of 1 implies a perfect agreement. This statistical score is represented by the following expression:

$$IoA = 1 - \frac{N\,(RMSE)^2}{\sum_{i=1}^{N}\left(\left|F-\overline{O}\right|+\left|O-\overline{O}\right|\right)^2} \qquad (1)$$

N represents the number of observations included in the calculation. *F* represents the simulated value and *O* the observation, while $\overline{O}$ corresponds to the time average observed. Besides, the average of the observed values and the average of the modelled values, for these variables and the wind direction, for graphical depiction purposes. In addition, for the wind direction variable, we have computed the root mean square error for the vector wind direction (RMSE-VWD).

The operational verification for all these meteorological variables has been carried out for all days of simulation independently: today, tomorrow and the day after tomorrow, and the winter of 2010-2011 and summer of 2011 seasons separately. Dividing the information for each day of simulation will permit us to evaluate the degree of the forecasts as the simulation progresses and define the model skill that will be expected from its initialization. Dividing the available data for each season of the year would permit us to evaluate the model skill in reproducing the meteorological characteristics within the Valencia Region for each season. Winter is defined by the months December-February while summer corresponds to June-August of the corresponding year. For each of these periods, the statistical scores for the meteorological magnitudes indicated above have been computed, on the one hand, merging all coastal stations and all inland stations separately, and on the other hand, merging all stations so as to provide a global analysis of the results.

Additionally, the operational verification has been applied to both versions of the model separately (RAMS44 and RAMS60). RAMS forecasts are released twice daily, at 0000 and 1200 UTC, for both simulations. However, the main information used by the forecasters to generate the forecast as well as to provide the RAMS products to the general public is that of the 0000 UTC simulations. Thus, in this paper, just the results obtained for this simulation will be presented, although similar results can be found for both simulations, as it was already pointed out in the case of evaluating the RAMS maximum and minimum temperature forecasts within the region of study (Gómez et al., 2013).

3. Results

3.1. Summer

In terms of processes and taking into account the results of temperature, it can be said that RAMS44 is capturing very well the daily heating for all sort of stations (Fig. 2a,b). Within the daily period of heating, the temperature observed and forecasted are really close to each other, and the same is found for the relative humidity, especially for inland stations. In contrast, the model is not capturing properly the daily cooling observed for these weather stations. As a consequence, the maximum temperature for coastal stations is quite well reproduced by the model, both in magnitude and occurrence, although slightly under-predicted. Moreover, the magnitude of the minimum temperature for these stations is rather well captured by the model. In this case, a delay of approximately one hour is observed. For inland stations, the model slightly overestimates the maximum temperature. Additionally, the minimum temperature is delayed by about one hour, with a model tendency to overestimate this magnitude. These results correspond as well with those found in Gómez et al. (2013).

In relation to RAMS60, the maximum temperature for all stations shows a tendency to underestimate the observations as well as the values provided by RAMS44. However, the daily minimum temperature captured by RAMS60 is a better estimation than that of RAMS44. In addition, the relative humidity for both versions of the model is rather similar at day-time. In contrast, RAMS60 produces higher relative humidity than RAMS44 during the night, producing the RAMS60 simulation to become closer to the observations. In general, the relative humidity presented by RAMS60 is higher than the values produced by RAMS44 for the whole day, although these differences are more significant at night.

During summer (Table 2), the IoA for the temperature is above 0.8 at day-time, with higher values for inland stations, indicating that RAMS is capturing the day-to-day and daily evolution properly. The bias computed for both sort of stations reflects the above comments on Fig. 2a,b: a positive bias inland and a negative one over the coast during the day. This statistic score shows an opposite trend between day and night. In general, the RMSE is lower for RAMS60, especially at night-time. For the relative humidity, the IoA offers values higher than 0.8 at day-time. Moreover, the bias shows a tendency to underestimate the observations. The RMSE is lower than 10% in general. However, the model presents more difficulties in forecasting the relative humidity for the RAMS44 simulation at night-time, showing the highest values of bias and RMSE.

Comparing the 2-m temperature with the near-surface temperature and the observations (Figs. 4a,b and 5a,b), we can see that the 2-m temperatures simulated by RAMS44 underestimate the observations for inland stations during the night (Fig. 4b). However, this magnitude is overestimated for coastal stations at day-time (Fig. 5a). It seems that the 2-m temperature computed by RAMS60 shows a better performance than the one on RAMS44.

The best results both in relative humidity and temperature are obtained in the first day of simulation. Thus, as the forecast moves forward, the magnitude of the difference between the observations and the simulation is more notable (not shown). Also Fig. 2a,b shows a slight descending trend as the simulation progresses.

In terms of the wind speed (Fig. 2c,d), both RAMS44 and RAMS60 overestimate this magnitude for the central period of the day and for both type of stations. However, the whole day is better capture by RAMS60. Furthermore, the model, in general, is able to capture the wind direction observed quite well. In contrast, RAMS60 shows more differences between the observations and the simulation for coastal stations. The period between 6:00 and 8:00 UTC shows the start of the transition between the land breeze observed at night and the sea breeze that is maintained during the day. RAMS is able to capture this regime wind flow transition very well in general, as it is also shown in the match between the observed and forecast wind speed and direction, especially using RAMS44. Also, this issue is clearly reproduced in the relative humidity hourly distribution (Fig. 2a,b).

In Table 3, we include the statistical scores for the wind speed and the RMSE-VWD. The evolution of the near-surface wind speed is better captured at night, when both RAMS44 and RAMS60 reproduce higher values of IoA, above 0.5. On the contrary, the model presents more difficulties in describing the observed values at day-time. In general, RAMS60 presents a better performance than RAMS44. This result is also reflected in the values of bias and RMSE for both stations. In Table 3, we may highlight the values of bias (0.12 ºC) and RMSE (about 1.0 ºC) produced by RAMS60 at 05 UTC. Similar results are also observed for RMSE-VWD.

Comparing the 10-m wind speed with the near-surface wind speed and the observations (Figs. 4c,d and 5c,d), we can see quite a explicit distribution of the day-time data (Fig. 5c,d). The variability included in these figures shows a gap between the four computed-variables (10-m wind speed and near-surface wind speed for both RAMS44 and RAMS60). As indicated previously in Fig. 2c,d, the model shows a tendency to overestimate the observations, especially at day-time and when applying RAMS44. However, the 10-m magnitude within the RAMS60 simulation reproduces the observations properly (Fig. 5c,d), presenting the best performance when compared with the measured wind speed.

3.2. Winter

During the winter season, one can find that the daily warming of RAMS is delayed compared to the observations (Fig. 3a,b), producing a delay in the maximum temperature and an underestimation of this magnitude, marked in the RAMS60 simulation. In contrast, the model is able to forecast the minimum temperature quite well, especially using RAMS60. In addition, it seems that the nocturnal cooling pattern is smoother compared to the other observations. As a result, the simulated temperatures overestimate the measurements within this period of the day. Contrasting the near-surface temperature produced by RAMS60 with that obtained with RAMS44, Fig. 3a,b , it shows lower value in the first case, for the whole simulation period and for both coastal and inland stations.

In the transition between the daytime heating and cooling, there are differences in relative humidity. With regard to this, it is observed how the model is increasing relative humidity causing a delay in this transition, while the observed relative humidity is stabilized earlier. Consequently, the daily heating is also delayed in the model compared to the observations, as mentioned before. In Fig. 3a,b it is shown that the differences between the observations and the simulation results become larger as the simulation progresses. These divergences are detected with both RAMS simulations.

However, opposite to the summer season, during the winter the model reproduces a slight increase tendency as the simulation moves forward.

Another dissimilarity discovered in the winter in relation to the summer is that the model produces a near-surface relative humidity that overestimates the observations, especially when using RAMS60. In contrast, the near-surface relative humidity is underestimated in the summer. In the case of wintertime, the differences between the observations and the forecasts are significantly reduced and the cooling does not follow the same pattern detected for the summer season. On the contrary, the minimum temperature is properly captured by RAMS44, while it remains slightly below the observations using RAMS60.

These results are also reflected in Table 4. It is shown that the model is able to capture quite well the daily evolution of the near-surface temperature and the inter-day progress of this magnitude, with a global IoA above 0.8 for all RAMS simulations. The bias score shows an opposite trend between day and night for this magnitude. Additionally, the daily evolution for relative humidity is quite well captured by the model during day-time, with more difficulties at night. If we compare the bias and RMSE for the near-surface relative humidity during winter and summer, it is observed that both scores are significantly reduced in winter compared to the values observed within the summer season.

Contrasting the 2-m temperature with the near-surface temperature and the observations (Figs. 6a,b and 7a,b), it has been found that the 2-m temperature simulated by RAMS44 underestimates the observations for inland stations both during night and day-time. However, this magnitude is overestimated for coastal stations during day-time. As within the summertime, the RAMS60 2-m temperature shows a better performance than the one from RAMS44.

In Fig. 3c,d, it is shown that the transition between the day and night flow is well captured by the model for both sort of stations. In this case, RAMS44 and RAMS60 provide similar results and are really close to the observations. In addition, comparing the wind speed magnitude, RAMS reproduces the measurements properly, with RAMS60 showing slightly lower values than those simulted by RAMS44.

In Table 5, one may see a general slight overestimation for the wind speed, lower than 1 m/s for both inland and coastal stations. The evolution of this magnitude is rather well captured by the model, with IoA above 0.7 in general. The RMSE wind speed remains in general below 2 m/s, with lower values for coastal stations and at night. Finally, as another contrast with the summer season, the RMSE-VWD during the winter shows no differences between day and night, nor between the two RAMS versions.

Comparing the winter near-surface wind speed with the 10-m wind speed (Figs. 6c,d and 7c,d), the results are not as clear as they are for the summer. In this case, it seems that there is greater variability during winter, not only at night and day-time, but also for both coastal and inland stations. This variability is observed in a larger dispersion of the data compared to the one observed within the summer season. These results could be related to a much more extended range of distinct meteorological situations during the winter.

4. Conclusions

The main aim of this paper has been to perform a verification of the operational forecasting system implemented in the Valencia Region, which has been established on different approaches. Firstly, the verification has been managed so as to compute the model skill by season of the year, specifically winter and summer. Secondly, two versions of the model have been implemented to use in the operational system. And, finally, the available information for the weather stations used in this study has been processed separately to distinguish between inland and coastal locations.

It has been shown that the main RAMS features for the summer season are a proper reproduction of the wind speed, especially using the RAMS60 simulation, and direction. Furthermore, the model is able to capture the daily heating very well. This has its implication while forecasting maximum temperatures. However, RAMS44 presents more difficulties in describing the nocturnal cooling observed. Thus, the model trend shows an over-estimation of the daily minimum temperature. In this case, RAMS60 predicts better the near-surface minimum temperature as well as the near-surface relative humidity observed. During the winter, we have seen that the model is able to capture the wind speed and direction properly, using the RAMS44 and the RAMS60 simulations. Moreover, RAMS is able to reproduce the daily cooling temperatures, although it presents more problems while dealing with the daily heating. These results have a direct impact on the maximum and minimum temperature forecasts. Both in summer and winter, RAMS60 shows a tendency to reproduce higher values of near-surface relative humidity and lower values of near-surface temperature than those simulated by RAMS44.

Comparing the summer and winter forecasts, it is shown that there is a larger variability for the last one. This result has been observed for all magnitudes analysed. It seems as if the forecast within the summer season was more stable than that simulated for the winter, indicating a likely different performance under distinct weather and atmospheric conditions. This is due to the fact that for the Valencia Region, and during the summer, mesoscale circulations are the predominant meteorological situations (Miró et al., 2009; Azorin-Molina, 2011). However, during the winter the most dominant situation is that associated with northerly-western circulations (Miró et al., 2009, Estrela et al., 2010). In this sense, it appears that during summer more similar meteorological conditions are observed, mainly connected with mesoscale circulation. On the contrary, distinct weather situations were recorded during winter, producing more variability. This has been highlighted especially considering the scatterplots for the wind speed, where the different RAMS simulations showed a concrete pattern within the summer, but produced greater variability in the winter season. Additionally, the RAMS44 near-surface wind speed shows the highest differences with the observations in the summer-time, while the RAMS60 10-m wind speed is suitable to represent the observed wind speed within this season of the year, especially at night-time.

Likewise, although the same model configuration has been maintained throughout the year, significant differences for the near-surface relative humidity have been observed between the simulation of the whole summer and winter seasons separately, with the last one providing more accurate results in this regard. Taking into account these findings, the relevance of the atmospheric humidity has been shown, as it has already been pointed out in several studies performed within other areas with Mediterranean-type climate regimes (Gershunov et al., 2009; Gershunov and Guirguis, 2012). Even though some differences have been detected between RAMS44 and RAMS60, a comparable trend is obtained in relation to the observations. Considering this issue, these RAMS results could also be associated with the initialization data and the boundary conditions provided by the GFS model to run RAMS. Besides, the differences distinguished between RAMS44 and RAMS60 could be linked to the change in the LEAF scheme used in both versions, which are responsible for the role of the energy budget between the atmosphere and the soil-vegetation surface. Unfortunately, the information needed to validate these questions is not available for this current study. Thus, it is the author's plan to investigate these questions in future research in addition to the introduction of upper air data to analyse the model performance at different heights and its impact on the surface results obtained here.

RAMS has been implemented for a concrete area within the Western Mediterranean Basin. However, due to its similar climate and physical characteristics, we strongly believe that the outcome of this study could be projected to other areas as well. In this sense, the results reproduced in the present paper are analogous to those found in other Mediterranean Regions, not only using the RAMS model (Pasqui et al., 2004; Federico, 2011), but also using other real-time mesoscale models (Bartzokas et al., 2010). On the contrary, the forecast temperature within the summer season presents a cold bias for the RAMS simulations over east-central Florida (Case et al., 2002). Regarding this subject, the results presented in the current work might also be useful, firstly, for researchers that plan to implement a mesoscale model operationally as presented in this paper, and secondly for researchers that already run this sort of system based on the RAMS model.

Finally, it must be said that the stations used in this study provide a detailed picture of the application of RAMS within the Valencia Region. We must also remark that, despite the implicit complexity of the implemented system and the limitations and constraints of such a system in terms of the ability to test diverse model parameters and factors that could positively affect the simulation results, it is very encouraging to notice that RAMS is able to reproduce the main patterns observed, on the whole, very well.

Acknowledgement

This work has been funded by the Regional Government of Valencia through the contract “Simulación de las olas de calor e invasiones de frío y su regionalización en la Comunitat Valenciana” (“Heat wave and cold invasion simulation and their regionalization at the Valencia Region”) and the project PROMETEO/2009/086. The authors wish to thank F. Pastor, J. Miró, M. J. Barberà and D. Corell for their appreciable collaboration. NCEP are acknowledged for providing the GFS meteorological forecasts for RAMS initialization.

References

Azorin-Molina C, Lopez-Bustins JA (2008). An automated sea breeze selection technique based on regional sea-level pressure difference: WeMOi. International Journal of Climatology 28: 1681–1692, doi: 10.1002/joc.1663.

Azorin-Molina C, Chen D, Tijm S, Baldi M (2011). A multi-year study of sea breezes in a Mediterranean coastal site: Alicante (Spain). International Journal of Climatology 31: 468–486, doi:10.1002/joc.2064.

Bartzokas A, Kotroni V, Lagouvardos K, Lolis CJ, Gkikas A, Tsirogianni MI (2010). Weather forecast in north-western Greece: RISKMED warnings and verification of mm5 model. Natural Hazards and Earth System Sciences 10:383-394.Besides, the observed averaged value and modelled averaged value are computed, for these variables and the wind direction, for graphical depiction purposes.”

Case JL Manobianco J, Dianic AV, Wheeler MM, Harms DE, Parks CR (2002). Verification of high-resolution rams forecasts over east-central Florida during the 1999 and 2000 summer months. Weather and Forecasting 17:1133-1151.

Chen C, Cotton WR (1983). A one-dimensional simulation of the stratocumulus-capped mixed layer. Boundary-Layer Meteorology 25:289-321.

Cotton WR, Pielke RAS, Walko RL, Liston GE, Tremback CJ, Jiang H, McAnelly RL, Harrington JY, Nicholls ME, Carrio GG, McFadden JP (2003). RAMS 2001: Current status and future directions. Meteorology and Atmospheric Physics 82 (1-4):5-29.

Estrela, MJ., Millán, MM., Peñarrocha, D y Pastor, F (2002). De la gota fría al frente de retroceso. Colección Interciencias. UNED, 260 pp. (In Spanish).

Estrela M, Pastor F, Miró J, Gómez I, Barberà M (2007). Heat waves prediction system in a mediterranean area (valencia region). 7th EMS Annual Meeting / 8th European Conference on Applications of Meteorology.

Estrela, MJ., Miró, J, Pastor, F, Millán, M (2010). Frontal Atlantic rainfall component in the Western Mediterranean Basin. Variability and spatial distribution. ESF-MedCLIVAR Workshop on “Hydrological, socioeconomic and ecological impacts of the North Atlantic Oscillation in the Mediterranean region”, Zaragoza (Spain), 24-27 May 2010.

Federico S (2011). Verification of surface minimum, mean, and maximum temperature forecasts in Calabria for summer 2008. Natural Hazards and Earth System Sciences 11: 487-500, doi:10.5194/nhess-11-487-2011.

Gangoiti, G, Millán, MM, Salvador, R, and Mantilla, E (2001). Long-range transport and re-circulation of pollutants in the western Mediterranean, during the project Regional Cycles of Air Pollution in the West-Central Mediterranean Area, Atmos. Environ., 35, 6267–6276.

Gershunov A, Cayan D, Iacobellis S (2009). The great 2006 heat wave over California and Nevada: Signal of an increasing trend. Journal of Climate 22: 6181-6203.

Gershunov A, Guirguis K (2012). California heat waves in the present and future. Geophysical Research Letters 39, L18710, doi:10.1029/2012GL052979.

Gómez I, Estrela MJ (2010). Design and development of a java-based graphical user interface to monitor/control a meteorological real-time forecasting system. Computers & Geosciences 36:1345-1354. doi:10.1016/j.cageo.2010.05.005.

Gómez I, Pastor F, Estrela MJ (2011). Sensitivity of a mesoscale model to different convective parameterization schemes in a heavy rain event. Natural Hazards and Earth System Sciences 11: 343-357, doi: 10.5194/nhess-11-343-2011.

Gómez I, Estrela, MJ, Caselles, V (2013). Operational forecasting of daily summer maximum and minimum temperatures in the Valencia Region. Natural Hazards 70(2): 1055-1076, doi: 10.1007/s11069-013-0861-1.

Gómez-Tejedor JA, Estrela MJ, Millán MM (1999). A mesoscale model application to fire weather winds. International Journal of Wildland Fire 9:255-263.

Mellor G, Yamada T (1982). Development of a turbulence closure model for geophysical fluid problems. Reviews of Geophysics and Space Physics 20:851-875.

Millán, M, Estrela, MJ, and Caselles, V (1995). Torrential Precipitations on the Spanish East Coast: The role of the Mediterranean Sea Surface Temperature, *Atmospheric Research* 36, 1–16.

Millán, MM, Salvador, R, Mantilla, E, and Kallos, G (1997). Photooxidants dynamics in the Mediterranean basin in summer: Results from European research projects, J. Geophys. Res., 102(D7), 8811–8823.

Millán, MM, Estrela MJ, y Miró, J (2005). Rainfall components: variability and spatial distribution in a Mediterranean area. *Journal of Climate* 18, 2682-2705.

Miró JJ, Estrela MJ, Millán MM (2006). Summer temperature trends in a mediterranean area (valencia region). International Journal of Climatology 26:1051-1073.

Miró J, Estrela MJ, Pastor F, Millán M (2009). Análisis comparativo de tendencias en la precipitación, por distintos inputs, entre los dominios hidrológicos del Segura y del Júcar (1958-2008), in Spanish. Investigaciones Geográficas 49: 129-157.

Molinari J. 1985. A general form of kuo's cumulus parameterization. Monthly Weather Review 113:1411-1416.

Palau JL, Pérez-Landa G, Diéguez JJ, Monter C, Millán MM (2005). The importance of meteorological scales to forecast air pollution scenarios on coastal complex terrain. Atmospheric Chemistry and Physics 5:2771-2785.

Pasqui M, Gioli B, Gozzini B, Miglietta F (2004). Atmospheric Regional Reanalysis simulations, based on RAMS model, as input for crop modelling. 26th Conference on Agricultural and Forest Meteorology.

Pastor F, Estrela MJ, Peñarrocha D, Millán MM (2001). Torrential rains on the spanish mediterranean coast. Modeling the effects of the sea surface temperature. Journal of Applied Meteorology 40(7):1180-1195.

Pastor F, Gómez I, Estrela MJ (2010). Numerical study of the october 2007 flash flood in the Valencia region (Eastern Spain): the role of orography. Natural Hazards and Earth System Science 10:1331-1345. doi:10.5194/nhess-10-1331-2010.

Pérez-Landa G, Ciais P, Sanz MJ, Gioli B, Miglietta F, Palau JL, Gangoiti G, Millán M (2007). Mesoscale circulations over complex terrain in the Valencia coastal region, Spain. Part 1: Simulation of diurnal circulation regimes. Atmospheric Chemistry and Physics 7:1835-1849.

Pielke Sr. RA (2002). Mesoscale meteorological modeling. 2nd Edition. Academic Press, San Diego, CA, 676 pp.

Salvador R, Millán M, Mantilla E, Baldasano JM. (1997). Mesoscale modelling of atmospheric processes over the western mediterranean area during summer. International Journal of Environment and Pollution 8:513-529.

Salvador R, Calbó J, Millán M (1999). Horizontal grid size selection and its influence on mesoscale model simulations. Journal of Applied Meteorology 39(9):1311-1329.

Tremback CJ, Walko RL, Bell MJ (2002). RAMS/HYPACT Evaluation and Visualization Utilities (REVU) user´s guide, version 2.3.1, Technical Report.

Walko RL, Cotton WR, Meyers MP, Harrington JY (1995). New RAMS cloud microphysics parameterization. Part I: The single-moment scheme. Atmospheric Research 38:29-62.

Walko RL, Band LE, Baron J, Kittel TGF, Lammers R, Lee TJ, Ojima D, Pielke RA, Taylor C, Tague C, Tremback CJ, Vidale PL (2000). Coupled atmospheric-biophysics-hydrology models for environmental modeling. Journal of Applied Meteorology 39:931-944.

Walko RL, Tremback CJ (2005). Modifications for the Transition From LEAF-2 to LEAF-3, ATMET Technical Note.

Willmott CJ (1981). On the validation of models. Physical Geography 2 (2):184-194.

Figure captions

Fig. 1. RAMS model domain configuration, and representative coastal and inland CEAM stations with orography of domain 3 (m).

Fig. 2. Measured (continuous line) and simulated (discontinuous line) near-surface temperature (ºC) and relative humidity (%) time series: coastal stations (a) and inland stations (b); near-surface wind direction (º) and wind speed (m/s): coastal stations (c) and inland stations (d), for both RAMS44 and RAMS60 configurations, the 2011 summer season and the 00 UTC RAMS cycle.

Fig. 3. Same as Fig. 2, but for the 2010-2011 winter season.

Fig. 4. Scatterplot of the simulated near-surface temperature (ºC) and 2-m temperature (ºC) at 05 UTC: coastal stations (a) and inland stations (b); near-surface wind speed (m/s) and 10-m wind speed (m/s): coastal stations (c) and inland stations (d), for both RAMS44 and RAMS60 configurations, within the 00 UTC RAMS cycle and the 2011 summer season, versus the corresponding measured magnitude.

Fig. 5. Same as Fig. 4, but at 13 UTC.

Fig. 6. Same as Fig. 4, but for the 2010-2011 winter season.

Fig. 7. Same as Fig. 5, but for the 2010-2011 winter season.

Tables

Table 1. Rams model settings for the three simulation grids: number of grid points in the x, y and z directions (nx, ny and nz), horizontal grid spacing (dx) and timestep (t).

Grid	nx	ny	nz	dx (m)	t (s)
1	83	58	24	48000	60
2	146	94	24	12000	30
3	78	126	24	3000	10

Table 2. Statistical scores for near-surface temperature and relative humidity, and 2-m temperature for the first day of simulation at 05 and 13 UTC, taken into account the 00 UTC RAMS initialization for versions 4.4 and 6.0 of the model and the 2011 summer season. Index of Agreement (IoA), Bias (ºC for temperature; % for relative humidity) and RMSE (ºC for temperature; % for relative humidity).

RAMS	Temperature			Relative Humidity			2-m Temperature		
	IoA	Bias	RMSE	IoA	Bias	RMSE	IoA	Bias	RMSE
Coastal Stations									
4.4 – 05Z	0.8	0.5	2	0.6	-4	19	0.9	0.4	1.9
4.4 – 13Z	0.9	-0.7	2	0.6	-6	14	0.5	5	6
6.0 – 05Z	0.8	-0.2	2	0.7	3	16	0.9	-0.5	1.8
6.0 – 13Z	0.8	-2	3	0.7	-2	12	0.9	1.6	3
Inland Stations									
4.4 – 05Z	0.7	3	4	0.4	-19	30	0.7	-5	6
4.4 – 13Z	0.9	1.0	3	0.7	-9	18	0.9	-0.4	4
6.0 – 05Z	0.7	1.9	4	0.5	-11	20	0.9	0.8	3
6.0 – 13Z	0.9	-0.6	3	0.8	-5	16	0.8	3	5
All Stations									
4.4 – 05Z	0.8	1.9	4	0.5	-14	24	0.8	-3	5
4.4 – 13Z	0.9	0.4	3	0.8	-8	17	0.8	1.5	5
6.0 – 05Z	0.8	1.2	3	0.6	-6	19	0.9	0.3	2
6.0 – 13Z	0.9	-1.1	3	0.8	-4	15	0.8	3	4

Table 3. Statistical scores for near-surface wind speed, 10-m wind speed and RMSE for the vector wind direction (VWD) for the first day of simulation at 05 and 13 UTC, taken into account the 00 UTC RAMS initialization for versions 4.4 and 6.0 of the model and the 2011 summer season. Index of Agreement (IoA), Bias (m/s), RMSE (m/s) and RMSE-VWD (m/s).

RAMS	Wind Speed			10-m Wind Speed			VWD
	IoA	Bias	RMSE	IoA	Bias	RMSE	RMSE
Coastal Stations							
4.4 – 05Z	0.7	0.5	1.3	0.7	0.14	1.0	2
4.4 – 13Z	0.4	3	3	0.5	1.6	2	4
6.0 – 05Z	0.8	-0.14	1.0	0.7	-0.5	1.0	1.8
6.0 – 13Z	0.6	1.5	1.8	0.8	0.15	0.9	3
Inland Stations							
4.4 – 05Z	0.6	1.0	1.6	0.6	0.5	1.2	3
4.4 – 13Z	0.4	2	3	0.5	0.8	2	5
6.0 – 05Z	0.6	0.8	1.5	0.6	0.4	1.2	2
6.0 – 13Z	0.6	1.2	2	0.6	0.06	1.7	4
All Stations							
4.4 – 05Z	0.6	0.9	1.5	0.6	0.4	1.2	2
4.4 – 13Z	0.4	2	3	0.5	1.1	2	5
6.0 – 05Z	0.6	0.5	1.4	0.6	0.12	1.1	2
6.0 – 13Z	0.6	1.3	2	0.7	0.09	1.4	4

Table 4. As in Table 2, but for the 2010-2011 winter season.

RAMS	Temperature			Relative Humidity			2-m Temperature		
	IoA	Bias	RMSE	IoA	Bias	RMSE	IoA	Bias	RMSE
Coastal Stations									
4.4 – 05Z	0.8	2	4	0.6	-11	22	0.9	1.0	3
4.4 – 13Z	0.9	-0.9	3	0.8	-0.4	18	0.8	1.9	4
6.0 – 05Z	0.9	1.3	3	0.8	-4	17	0.9	0.3	3
6.0 – 13Z	0.8	-2	3	0.8	5	17	0.9	-0.6	3
Inland Stations									
4.4 – 05Z	0.7	3	5	0.5	-10	24	0.7	-5	6
4.4 – 13Z	0.9	-1.1	3	0.9	3	16	0.8	-4	6
6.0 – 05Z	0.8	2	5	0.6	-3	20	0.9	0.4	3
6.0 – 13Z	0.9	-2	4	0.8	8	16	0.9	-1.0	3
All Stations									
4.4 – 05Z	0.8	3	5	0.6	-10	24	0.8	-3	5
4.4 – 13Z	0.9	-1.0	3	0.8	1.9	16	0.8	-2	5
6.0 – 05Z	0.9	1.8	4	0.7	-4	19	0.9	0.4	3
6.0 – 13Z	0.9	-2	3	0.8	7	16	0.9	-0.8	3

Table 5. As in Table 3, but for the 2010-2011 winter season.

RAMS	Wind Speed			10-m Wind Speed			VWD
	IoA	Bias	RMSE	IoA	Bias	RMSE	RMSE
Coastal Stations							
4.4 – 05Z	0.8	0.8	1.8	0.8	0.18	1.6	3
4.4 – 13Z	0.8	0.6	2	0.8	-0.08	1.7	3
6.0 – 05Z	0.8	0.18	1.5	0.8	-0.4	1.5	3
6.0 – 13Z	0.8	0.06	1.8	0.7	-0.7	1.8	3
Inland Stations							
4.4 – 05Z	0.8	0.4	1.9	0.7	-0.2	1.8	3
4.4 – 13Z	0.7	-0.003	2	0.7	-0.8	2	3
6.0 – 05Z	0.8	0.4	1.8	0.8	-0.16	1.7	3
6.0 – 13Z	0.8	-0.2	1.9	0.7	-0.9	2	3
All Stations							
4.4 – 05Z	0.8	0.5	1.9	0.8	-0.08	1.7	3
4.4 – 13Z	0.7	0.2	2	0.7	-0.5	2	3
6.0 – 05Z	0.8	0.3	1.7	0.8	-0.3	1.6	3
6.0 – 13Z	0.8	-0.13	1.9	0.7	-0.9	2	3

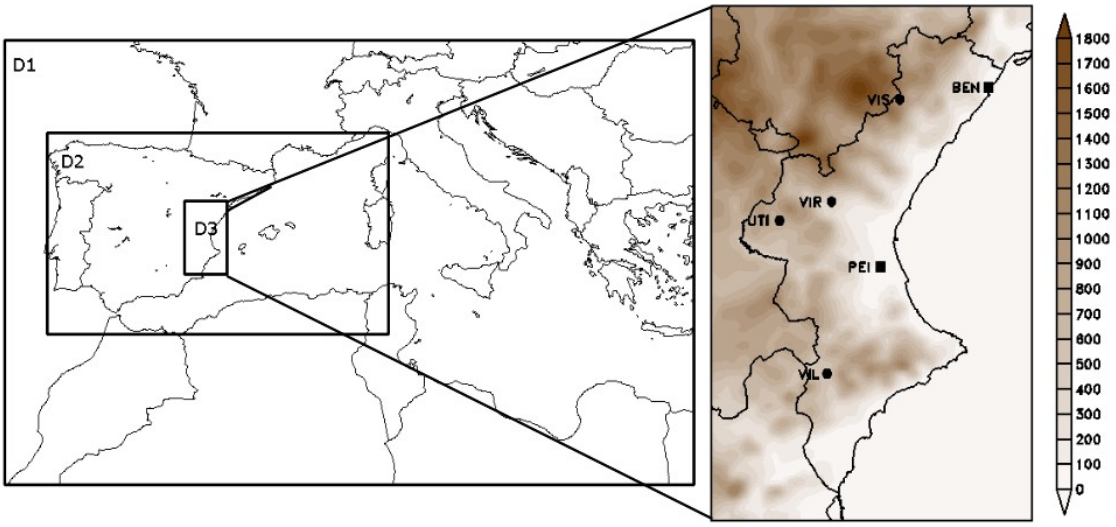

Fig. 1. RAMS model domain configuration, and representative coastal and inland CEAM stations with orography of domain 3 (m).

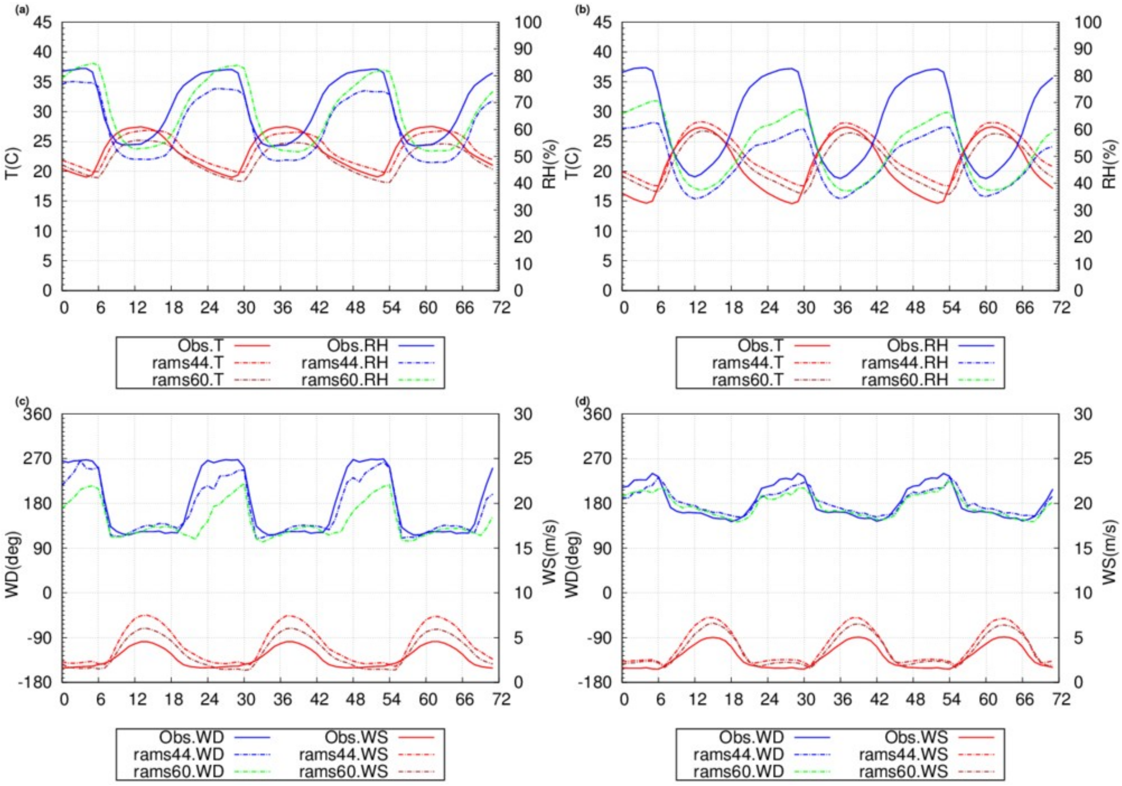

Fig. 2. Measured (continuous line) and simulated (discontinuous line) near-surface temperature (ºC) and relative humidity (%) time series: coastal stations (a) and inland stations (b); near-surface wind direction (º) and wind speed (m/s): coastal stations (c) and inland stations (d), for both RAMS44 and RAMS60 configurations, the 2011 summer season and the 00 UTC RAMS cycle.

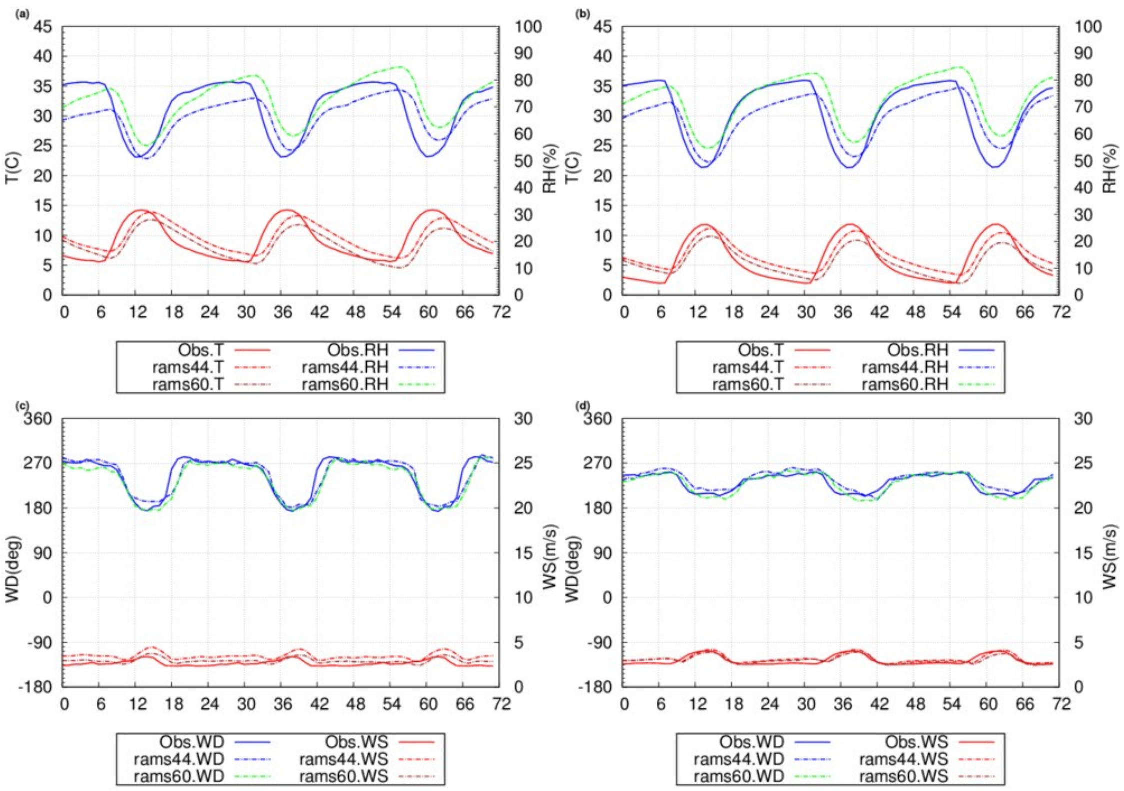

Fig. 3. Same as Fig. 2, but for the 2010-2011 winter season.

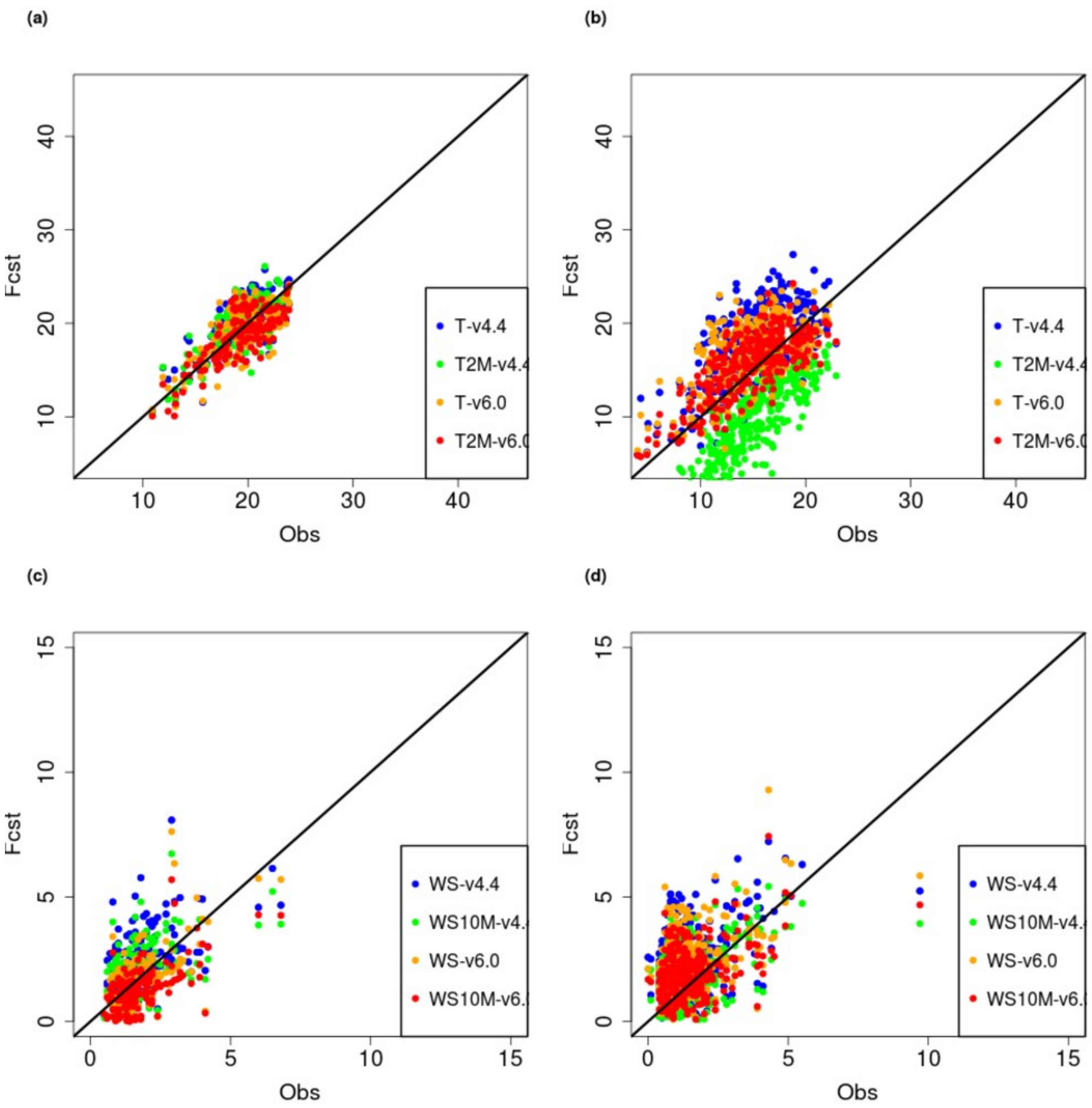

Fig. 4. Scatterplot of the simulated near-surface temperature (ºC) and 2-m temperature (ºC) at 05 UTC: coastal stations (a) and inland stations (b); near-surface wind speed (m/s) and 10-m wind speed (m/s): coastal stations (c) and inland stations (d), for both RAMS44 and RAMS60 configurations, within the 00 UTC RAMS cycle and the 2011 summer season, versus the corresponding measured magnitude.

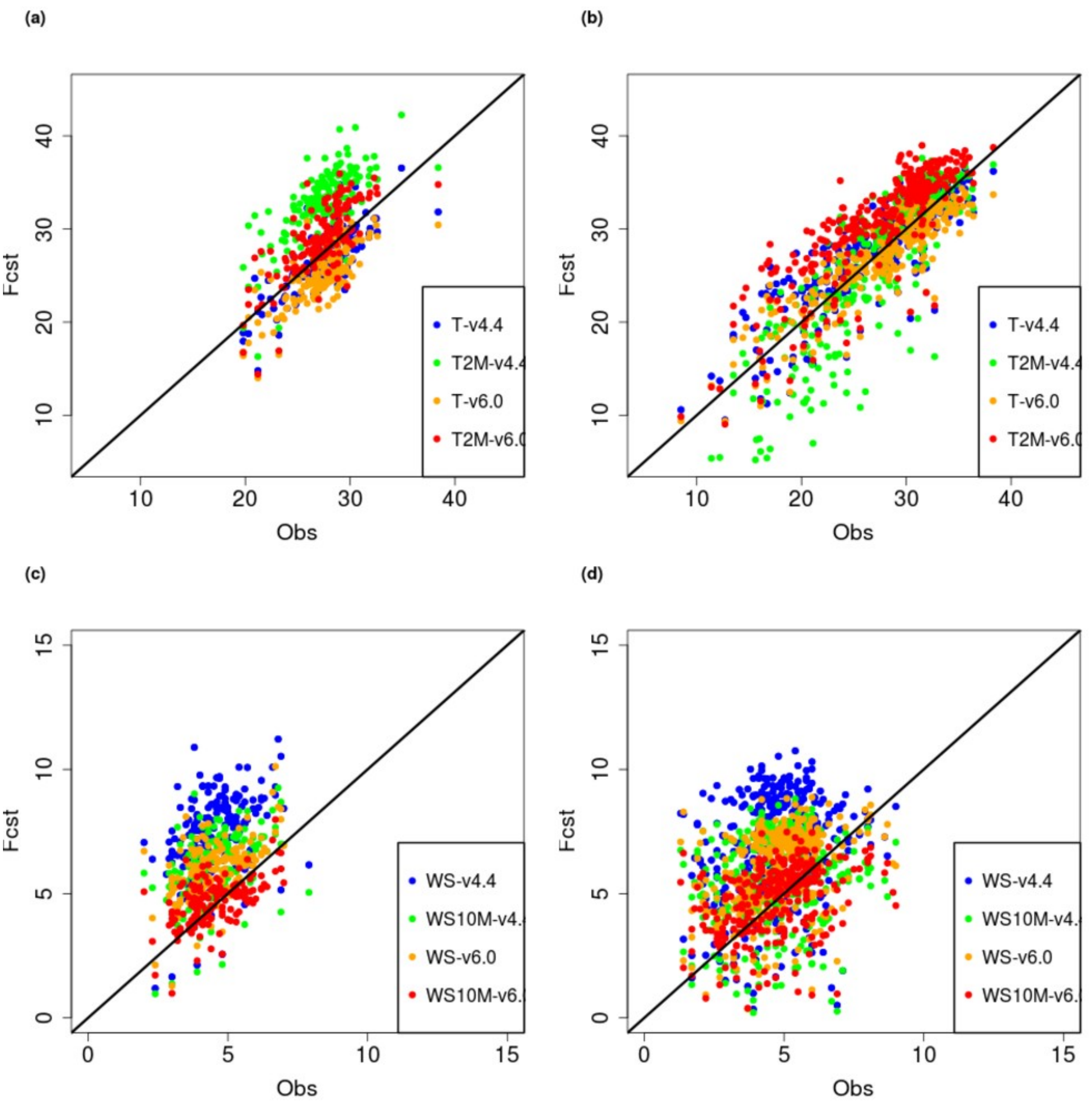

Fig. 5. Same as Fig. 4, but at 13 UTC.

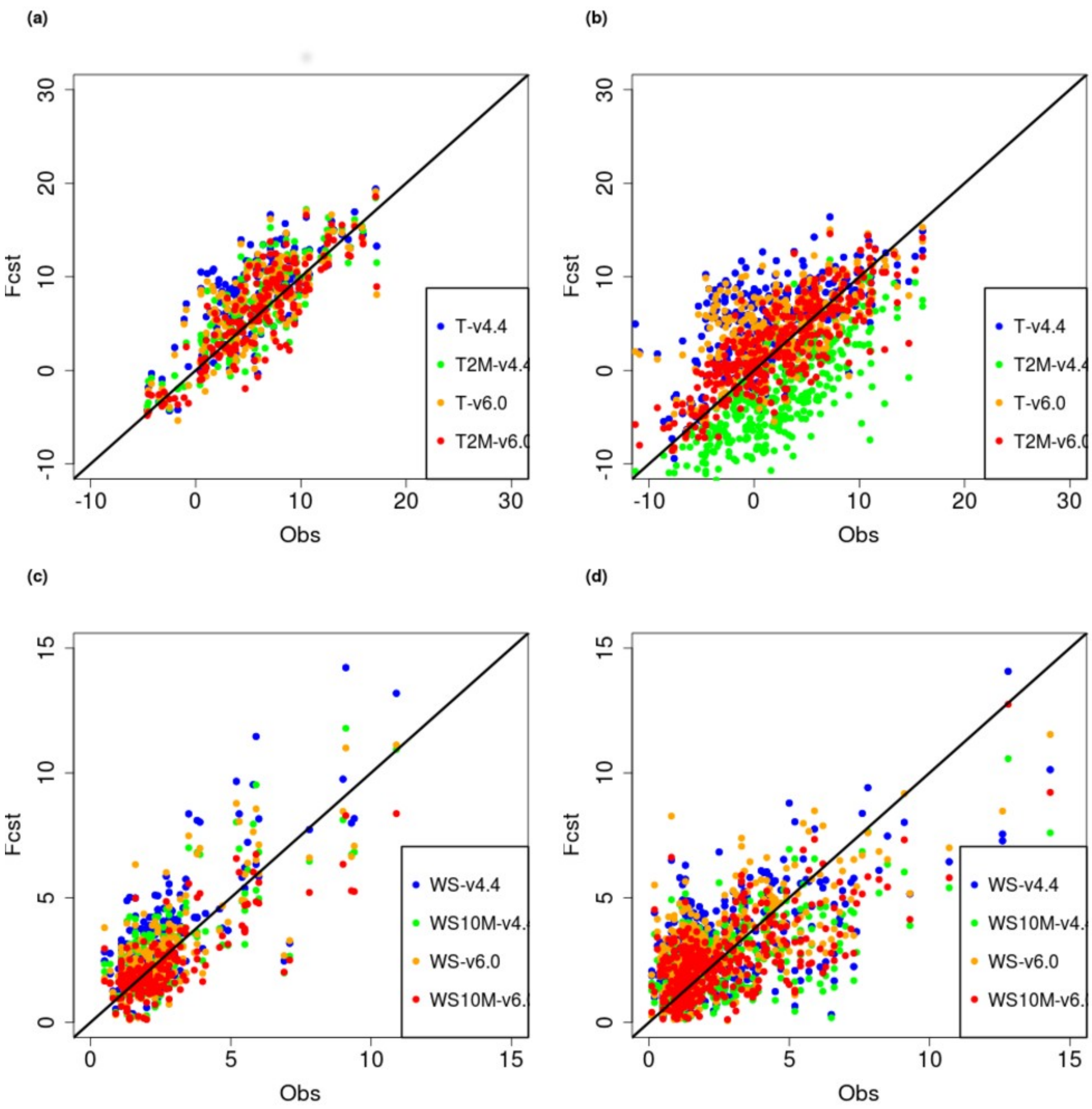

Fig. 6. Same as Fig. 4, but for the 2010-2011 winter season.

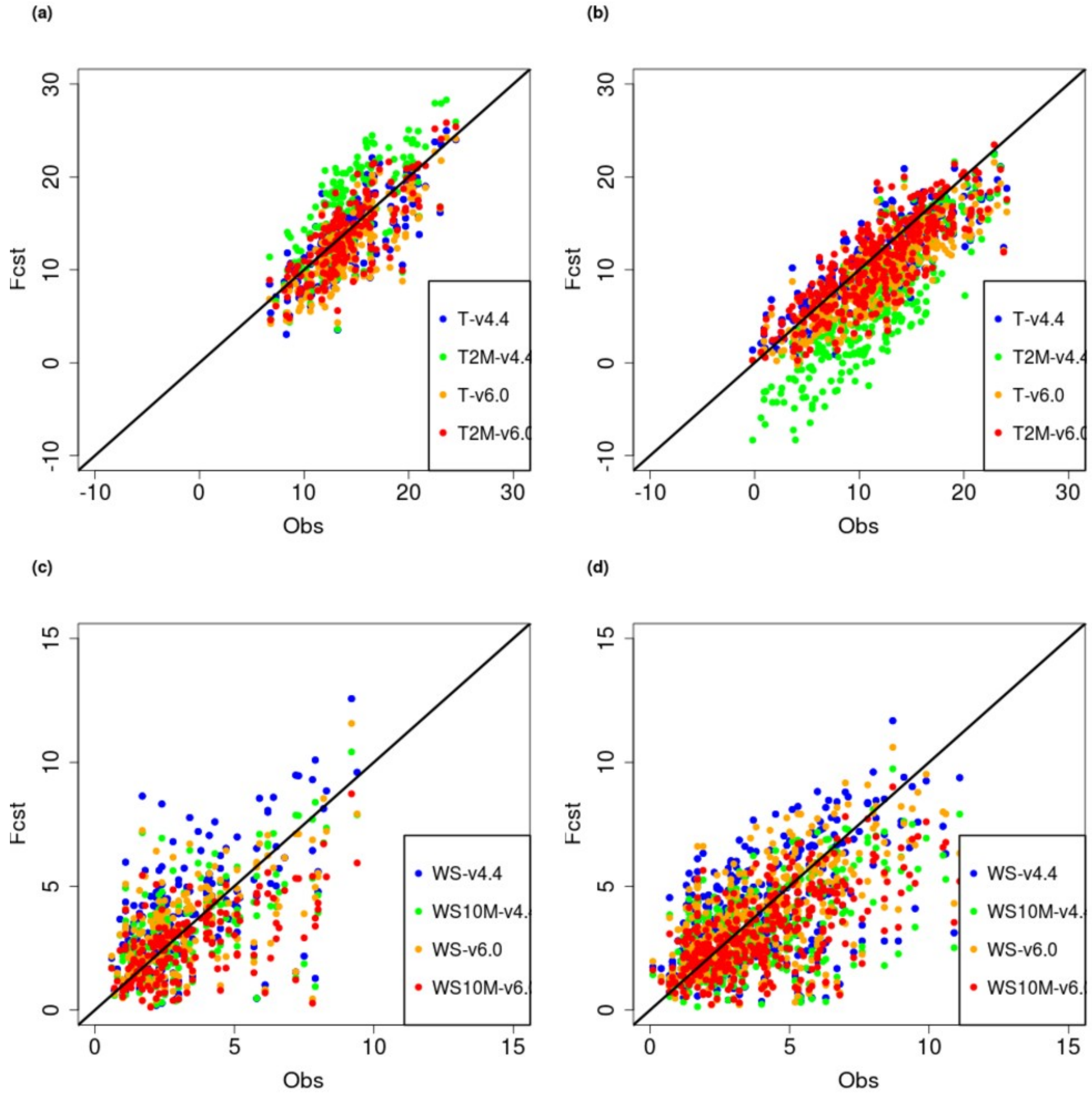

843Fig. 7. Same as Fig. 5, but for the 2010-2011 winter season.